Comments to the author:

One of the reviewers have a minor follow-up comment that they hope you will address: Lines 118–122: It is not "a given" that the solvent extract absorbance is not converted to particulate absorption with Mie calculations; certain studies have attempted this conversion. What could be highlighted in this sentence is that even in this case, pH and solvent matrix effects, as well as the potential incomplete solubility of BrC in common solvents, should still be considered in order to be able to reliably compare BrC absorption measured directly in particles vs. that derived from solvent extracts (with Mie calculations). I suggest rephrasing to remove ambiguity.

Reply:

The original expression was changed to

"Even when the solvent extract absorption is converted to particulate absorption with Mie calculations, pH and solvent matrix effects, as well as the potential incomplete solubility of BrC in common solvents, should still be considered before comparing BrC absorption measured directly in particles versus that derived from solvent extracts." (Lines 118 – 122)

Potential underestimation of ambient brown carbon absorption based on the methanol extraction method and its impacts on source analysis

Zhenqi Xu[a], Wei Feng[a], Yicheng Wang[a], Haoran Ye[a], Yuhang Wang[b], Hong Liao[a], Mingjie Xie[a,*]

[a]Collaborative Innovation Center of Atmospheric Environment and Equipment

Technology, Jiangsu Key Laboratory of Atmospheric Environment Monitoring and

Pollution Control, School of Environmental Science and Engineering, Nanjing

University of Information Science & Technology, 219 Ningliu Road, Nanjing 210044,

China

[b]School of Earth and Atmospheric Sciences, Georgia Institute of Technology, Atlanta,

GA 30332, United States

*Corresponding to:

Mingjie Xie (mingjie.xie@nuist.edu.cn, mingjie.xie@colorado.edu);

Mailing address: 219 Ningliu Road, Nanjing, Jiangsu, 210044, China

Abstract

The methanol extraction method was widely applied to isolate organic carbon (OC) from ambient aerosols, followed by measurements of brown carbon (BrC) absorption. However, undissolved OC fractions will lead to underestimated BrC absorption. In this work, water, methanol (MeOH), MeOH/dichloromethane (MeOH/DCM, 1:1, v/v), MeOH/DCM (1:2, v/v), tetrahydrofuran (THF), and N,N-dimethylformamide (DMF) were tested for extraction efficiencies of ambient OC, and the light absorption of individual solvent extracts was determined. Among the five solvents and solvent mixtures, DMF dissolved the highest fractions of ambient OC (up to ~95%), followed by MeOH and MeOH/DCM mixtures (< 90%), and the DMF extracts had significant ($p < 0.05$) higher light absorption than other solvent extracts. This is because the OC fractions evaporating at higher temperatures (> 280°C) are less soluble in MeOH (~80%) than in DMF (~90%) and contain stronger light-absorbing chromophores. Moreover, the light absorption of DMF and MeOH extracts of collocated aerosol samples in Nanjing showed consistent temporal variations in winter when biomass burning dominated BrC absorption. While the average light absorption of DMF extracts was more than two times greater than the MeOH extracts in late spring and summer. The average light absorption coefficient at 365 nm of DMF extracts was 30.7% higher ($p < 0.01$) than that of MeOH extracts. Source apportionment results indicated that the MeOH solubility of BrC associated with biomass burning, lubricating oil combustion, and coal combustion is similar to their DMF solubility. The BrC linked with unburned fossil fuels and polymerization processes of aerosol organics was less soluble in MeOH than in DMF, which was likely the main reason for the large difference in time series between MeOH and DMF extract absorption. These results highlight the importance of testing different solvents to investigate the structures and light absorption of BrC,

2

53   particularly for the low-volatility fraction potentially originating from non-combustion

54   sources.

55

56

57

58

59

60

61

62

63

64

65

66

67

68

69

70

71

72

73

74

75

76

77

1 Introduction

Besides black carbon (BC) and mineral dust, growing evidence shows that organic carbon (OC) aerosols derived from various combustion sources (e.g., biofuel and fossil fuel) and secondary processes (e.g., gas-phase oxidation, aqueous and in-cloud processes) can absorb sunlight at short visible and UV wavelengths (Laskin et al., 2015; Hems et al., 2021). The radiative forcing (RF) of the light-absorbing organic carbon, also termed "brown carbon" (BrC), is not well quantified due to the lack of its emission data, complex secondary formations, and large uncertainties in *in situ* BrC measurements (Wang et al., 2014; Wang et al., 2018; Saleh, 2020). The imaginary part of the refractive index (k) of BrC is required when modeling its influence on aerosols direct RF, and is retrieved by the optical closure method combing online monitoring of aerosol absorption and size distributions with Mie theory calculations (Lack et al., 2012; Saleh et al., 2013; Saleh et al., 2014). However, several pre-assumptions must be made on aerosol morphology (spherical Mie model) and mixing states of BC and organic aerosols (OA), which might introduce large uncertainties in the estimation of k (Mack et al., 2010; Xu et al., 2021).

To improve the understanding on chemical composition and light-absorbing properties of BrC chromophores, organic matter (OM) in aerosols was isolated through solvent extraction using water and/or methanol, followed by filtration and a series of instrumental analysis (e.g., UV/Vis spectrometer, liquid chromatograph-mass spectrometer; Chen and Bond, 2010; Liu et al., 2013; Lin et al., 2016). Referring to existing studies, a larger fraction of the methanol extract absorption comes from water-insoluble OM containing conjugated structures (Chen and Bond, 2010; Huang et al., 2020); the light absorption of biomass burning OM is majorly contributed by large molecules (MW > 500~1000 Da; Di Lorenzo and Young, 2016; Di Lorenzo et al., 2017)

103 and depends on burn conditions (Saleh et al., 2014); polycyclic aromatic hydrocarbons

104 (PAHs) and nitroaromatic compounds (NACs) are ubiquitous BrC chromophores in the

105 atmosphere (Huang et al., 2018; Wang et al., 2019), but the identified species only

106 explain a few percentages (< 10%) of total BrC absorption (Huang et al., 2018; Li et

107 al., 2020).

108 Methanol can extract > 90% OM from biomass burning (Chen and Bond, 2010;

109 Xie et al., 2017b), while the extraction efficiency (η, %) decreases to ~80% for ambient

110 organic aerosols (Xie et al., 2019b; Xie et al., 2022) possibly due to other sources

111 emitting large hydrophobic molecules and oligomerizations of small molecules during

112 the aging process (Cheng et al., 2021; Li et al., 2021). The light-absorbing properties

113 and structures of methanol-insoluble OC (MIOC) are still unknown. By comparing BrC

114 characterization results of offline and online methods, some studies conclude that the

115 MIOC dominates BrC absorption in source and ambient aerosols (Bai et al., 2020; Atwi

116 et al., 2022). However, the online-retrieval and offline-extraction methods are designed

117 based on different instrumentation and purposes, and the online method depends largely

118 on presumed and uncertain optical properties of BC (Wang et al., 2014). Even when the

119 solvent extract absorption is converted to particulate absorption with Mie calculations,

120 pH and solvent matrix effects, as well as the potential incomplete solubility of BrC in

121 common solvents, should still be considered before comparing BrC absorption

122 measured directly in particles versus that derived from solvent extracts. ~~Given that the~~

123 ~~solvent extract absorption is not converted to particulate absorption with Mie~~

124 ~~calculations, solvent and pH effects are not accounted for, and BrC is not completely~~

125 ~~dissolved in typical solvents (e.g., water and methanol), BrC absorption in particles and~~

126 ~~solution can hardly be compared directly.~~ To reveal the absorption and composition of

127 MIOC, it is necessary to find a new solvent or develop a new methodology to improve

5

128   OC extraction efficiency (Shetty et al., 2019).

129   In this work, a series of single solvents and solvent blends were tested for extraction

130   efficiencies of OC in ambient particulate matter with aerodynamic diameter < 2.5 μm

131   (PM$_{2.5}$), and the sample extract absorption of each solvent was compared. The solvent

132   or solvent mixture with the highest η value was applied to extract a matrix of collocated

133   PM$_{2.5}$ samples followed by light absorption measurements. In our previous work, the

134   light absorption of methanol extracts of the same samples was measured, and source

135   apportionment was performed using organic molecular marker data (Xie et al., 2022).

136   By comparing with the study results in Xie et al. (2022), this study evaluated potential

137   underestimation of BrC absorption in methanol and its impacts on BrC source

138   attributions. These results suggest that different solvents should be used in future

139   investigations on the absorption, composition, sources, and formation pathways of low-

140   volatility BrC.

141   **2. Methods**

142   *2.1 Solvent selection*

143   Five solvents and solvent mixtures including water, methanol (MeOH),

144   MeOH/dichloromethane (MeOH/DCM, 1:1, v:v), MeOH/DCM (1:2, v:v),

145   tetrahydrofuran (THF), and N,N-dimethylformamide (DMF) were selected to extract

146   OC from identical PM$_{2.5}$ samples to determine which solvent or solvent mixture has the

147   highest η value. Water and methanol are the most commonly used solvents to extract

148   BrC from source or ambient particles. Cheng et al. (2021) found that OC produced

149   through the combustion of toluene, isooctane, and cyclohexane were more soluble in

150   DCM than MeOH. Since a major part of BrC absorption is coming from unknown large

151   molecules (Di Lorenzo and Young, 2016; Di Lorenzo et al., 2017), polar aprotic

152   solvents THF and DMF were tested due to their high capacity for dissolving large

6

153 polymers. Except for water and MeOH, DCM and THF were rarely used to extract OC

154 for light absorption measurements (Cheng et al., 2021; Moschos et al. 2021), and DMF

155 has not ever been tested for extracting BrC in literature.

156 *2.2 Sampling*

157 **Sampling for solvent test.** To compare OC extraction efficiencies and extract

158 absorption of the five selected solvents and solvent mixtures, twenty-one ambient $PM_{2.5}$

159 samples were collected on the rooftop of a seven-story library building in Nanjing

160 University of Information Science and Technology (NUIST, 32.21ºN, 118.71ºE).

161 Details of the sampling site and equipment were provided by Yang et al. (2021). Two

162 identical mid-volume samplers (Sampler I and II; $PM_{2.5}$-PUF-300, Mingye

163 Environmental, China) equipped with 2.5 μm cut-point impactors were used for

164 ambient air sampling during day-time (8:00 a.m.–7:00 p.m.) and night-time (8:00 p.m.–

165 7:00 a.m. the next day), respectively, in December 2019. After the impactor, $PM_{2.5}$ in

166 the air stream was collected on a pre-baked (550 °C, 4 h) quartz filter (20.3 cm ×12.6

167 cm, Munktell Filter AB, Sweden) at a flow rate of 300 L min^{-1}. $PM_{2.5}$ filter and field

168 blank samples were sealed and stored at –20 °C before chemical analysis. Information

169 about $PM_{2.5}$ samples for the solvent test is provided in Table S1 of supplementary

170 information.

171 **Ambient sampling for BrC analysis.** Details of the ambient sampling were described

172 in previous work (Qin et al., 2021; Yang et al., 2021; Xie et al., 2022). Briefly, Sampler

173 I and II were equipped with two quartz filters in series (quartz behind quartz, QBQ

174 method; Q_f and Q_b) followed by adsorbents. Collocated filter and adsorbent samples

175 were collected every sixth day during daytime and nighttime from 2018/09/28 to

176 2019/09/28. Field blank sampling was performed every 10th sample to address

177 contamination. Q_f samples loaded with $PM_{2.5}$ were speciated and extracted for light

178 absorption measurements. The OC adsorbed on Q_b and its light absorption were

179 analyzed to determine positive sampling artifacts. The adsorbents in sampler I [a

180 polyurethane foam (PUF)/XAD-4 resin/PUF sandwich] and II (a PUF plug) were used

181 to collect gas-phase nonpolar and polar organic compounds, respectively. The

182 measurement results of gas- and particle-phase organic compounds were provided by

183 Gou et al. (2021) and Qin et al. (2021).

184 *2.3 Solvent test for light absorption and extraction efficiency*

185   An aliquot (~6 cm^2) of each filter sample was extracted ultrasonically in 10 mL of

186 each solvent or solvent mixture (HPLC grade) for 30 min (one-time extraction

187 procedure, $N = 11$; Table S1). After filtration, the light absorbance (A_λ) of individual

188 solvent extracts was measured over 200–900 nm using a UV/Vis spectrometer (UV-

189 1900, Shimadzu Corporation, Japan), and was converted to light absorption coefficient

190 (Abs_λ, Mm^{-1}) by

191 $$Abs_\lambda = (A_\lambda - A_{700}) \times \frac{V_l}{V_a \times L} \ln(10) \qquad (1)$$

192 where A_{700} is subtracted to correct baseline drift, V_l (m^3) is the air volume of the

193 extracted sample, L (0.01 m) is the optical path length, and ln (10) was multiplied to

194 transform Abs_λ from a common to a natural logarithm (Hecobian et al., 2010). To

195 understand if multiple extractions could draw out more BrC, a two-time extraction

196 procedure was applied for another 10 ambient PM$_{2.5}$ samples in the same manner (Table

197 S1). The A_λ of the 1st and 2nd extractions (10 mL each) was measured separately for

198 Abs_λ calculations.

199   Prior to solvent extractions, the concentrations of OC and EC in each filter sample

200 were analyzed using a thermal-optical carbon analyzer (DRI, 2001A, Atmoslytic,

201 United States) following the IMPROVE-A protocol. OC and EC were converted to CO_2

step by step during two separate heating cycles [OC1 (140°C) – OC2 (280°C) – OC3 (480°C) – OC4 (580°C) in pure He, EC1 (580°C) – EC2 (740°C) – EC3 (840°C) in 98% He/2% O_2], and the emitted CO_2 during each heating step was converted to CH_4 and measured using a flame ionization detector (FID).

After extractions, filters extracted by MeOH, MeOH/DCM (1:1), MeOH/DCM (1:2), and THF were air-dried in a fume hood and analyzed for residual OC (rOC, µg m^{-3}) using the identical method. Filters extracted in water and DMF cannot be air-dried in the short term due to the low volatility of solvents, and their rOC was measured after baking at 100 °C for 2 h. The total amount of OC dissolved in water for each sample was also measured as water-soluble OC (WSOC) by a total organic carbon analyzer (TOC-L, Shimadzu, Japan; Yang et al., 2021). To examine if the baking process would influence rOC measurements, the rOC of filters extracted in MeOH, MeOH/DCM mixtures, and THF were also measured after the baking process and compared to those determined after air dried. The pyrolytic carbon (PC) was used to correct for sample charring and was determined when the filter transmittance or reflectance returned to its initial value during the analysis (Schauer et al., 2003), but the formation of PC is very scarce when analyzing extracted filters. In this study, solvent-extractable OC (SEOC, µg m^{-3}) was determined by the difference in OC1–OC4 between pre- and post-extraction samples. The extraction efficiency (η, %) of each solvent was expressed as

$$\eta = \frac{\text{SEOC}}{\text{OC}} \times 100\% \qquad (2)$$

Here, SEOC denotes WSOC when the solvent is water. For the ambient samples extracted twice, rOC was measured only after the two-extraction procedure was completed.

The solution mass absorption efficiency (MAE$_\lambda$, m^2 g^{-1} C) was calculated by dividing Abs$_\lambda$ by the concentration of SEOC

227 $$MAE_\lambda = \frac{Abs_\lambda}{SEOC} \qquad (3)$$

228 and the solution absorption Ångström exponent (Å), a parameter showing the

229 wavelength dependence of solvent extract absorption, was obtained from the regression

230 slope of lg (Abs$_\lambda$) versus lg (λ) over 300–550 nm.

231   The solvent effect is not uncommon when measuring aerosol extract absorbance in

232 difference solvents (Chen and Bond, 2010; Mo et al., 2017; Moschos et al., 2021), but

233 is rarely accounted for in previous studies. To evaluate the influence of solvent effects

234 on light absorption of different solvent extracts of the same sample, solutions of 4-

235 nitrophenol at 1.90 mg L^{-1}, 4-nitrocatechol at 1.84 mg L^{-1}, and 25-PAH mixtures (Table

236 S2) at 0.0080 mg L^{-1} and 0.024 mg L^{-1} (each species) in the five solvents and solvent

237 mixtures were made up for five times and analyzed for UV/Vis spectra. The absorbance

238 of PAH mixtures in water was not provided due to their low solubility.

239 *2.3 Measurements and analysis of ambient BrC absorption*

240   Collocated Q$_f$ and Q$_b$ samples were extracted using the solvent with the highest η

241 value once followed by light absorbance measurement. OC concentrations in Q$_f$ and Q$_b$

242 samples were obtained from Yang et al. (2021), and SEOC values were estimated from

243 OC concentrations and the average η value determined in *section 2.1* for one-time

244 extraction. In this work, Q$_b$ measurements were used to correct Abs$_\lambda$, MAE$_\lambda$, and Å of

245 BrC in ambient PM$_{2.5}$ in the same manner as those for water and methanol extracts in

246 Xie et al. (2022)

247 $$\text{Artifact-corrected } Abs_\lambda = Abs_\lambda^{Qf} - Abs_\lambda^{Qb} \qquad (4)$$

248 $$\text{Artifact-corrected } MAE_\lambda = \frac{Abs_\lambda^{Qf} - Abs_\lambda^{Qb}}{SEOC_{Qf} - OC_{Qb}} \qquad (5)$$

249 where Abs$^{Qf}_\lambda$ and Abs$^{Qb}_\lambda$ are Abs$_\lambda$ values of Q$_f$ and Q$_b$ samples, respectively; SEOC$_{Qf}$

250 represents SEOC concentrations in Q$_f$ samples; OC$_{Qb}$ denotes OC concentrations in Q$_b$

251 samples, assuming that OC in Q_b is completely dissolved (Xie et al., 2022). Artifact

252 corrected Å were generated from the regression slope of lg (Abs^{Qf}_λ - Abs^{Qb}_λ) versus lg

253 (λ) over 300 – 550 nm. Artifact-corrected Abs_λ, MAE_λ, and Å during each sampling

254 interval were determined by averaging each pair of collocated measurements. If one of

255 the two numbers in a pair is missed, the other number will be directly used for the

256 specific sampling interval. To compare with previous studies based on water and/or

257 methanol extraction methods, Abs_λ and MAE_λ at 365 nm were shown and discussed in

258 this work.

259   Pearson's correlation coefficient (r) was used to show how collocated

260 measurements of BrC in ambient $PM_{2.5}$ vary together. The coefficient of divergence

261 (COD) was calculated to indicate consistency between collocated measurements. The

262 relative uncertainty of BrC absorption derived from duplicate data was depicted using

263 the average relative percent difference (ARPD, %), which was used as the uncertainty

264 fraction for BrC measurements. Calculation methods of COD and ARPD are provided

265 in Text S1 of supplementary information. To examine the influence of potential BrC

266 underestimation based on the methanol extraction method on source apportionment,

267 positive matrix factorization (PMF) version 5.0 (U.S. Environmental Protection

268 Agency) was applied to attribute the light absorption of aerosol extracts in methanol

269 and solvent with the highest η to sources. The total concentration data (Q_f + Q_b +

270 adsorbent) of organic compounds have been used to apportion the light absorption of

271 MeOH-soluble OC to specific sources (Xie et al., 2022), so as to avoid the impacts of

272 gas-particle partitioning. In this work, the input particulate bulk components and total

273 organic molecular marker (OMM) data for PMF analysis were obtained from Xie et al.

274 (2022) and are summarized in Table S3. Four- to ten-factor solutions were tested to

275 retrieve a final factor number with the most physically interpretable base-case solution.

276 More information on input data preparation and the factor number determination are

277 provided in supplementary information (Text S2 and Table S4).

278 **3. Results and discussion**

279 *3.1 Solvent test*

280 3.1.1 Extraction efficiency of different solvents

281   The concentrations of OC and EC fractions in each sample prior to solvent

282 extractions are listed in Table S1. SEOC concentrations and extraction efficiencies of

283 individual solvents and solvent mixtures are detailed in Table 1. Generally, DMF

284 presented the highest extraction efficiency of total OC whenever filter samples were

285 extracted once ($89.0 \pm 7.96\%$) or twice ($95.6 \pm 3.67\%$), followed by MeOH (one-time

286 extraction $82.3 \pm 8.68\%$, two-time extraction $86.6 \pm 7.86\%$) and MeOH/DCM mixtures

287 ($\sim 75\%$, $\sim 85\%$). Although THF and DMF are frequently used to dissolve polymers (e.g.,

288 polystyrene) for characterization, THF had the lowest η values ($64.2 \pm 8.08\%$, $70.1 \pm$

289 8.01%) comparable to water ($66.7 \pm 8.58\%$, $69.9 \pm 5.88\%$). Compared with one-time

290 extraction, the extraction efficiencies of selected solvents were improved by a few

291 percent when filter samples were extracted twice, and η values of MeOH/DCM

292 mixtures became closer to those of MeOH (Table 1). These results showed that solvents

293 can reach more than 80% of their dissolving capacity with the one-time extraction, and

294 the ambient OC in Nanjing is more soluble in MeOH than in DCM.

295   From OC1 to OC4, the volatility of OC fractions is expected to decrease

296 continuously, and the molecules in OC fractions evolving at higher temperatures should

297 be larger than those in OC1 with similar functional groups. In Table 1, MeOH and

298 MeOH/DCM mixtures had comparable or even higher η values ($82.6 \pm 25.9\%$–$97.9 \pm$

299 5.02%) of OC1 and OC2 than DMF ($88.8 \pm 4.98\%$–$97.2 \pm 2.12\%$). But OC3 and OC4

300 accounted for more than 60% of OC concentrations, and DMF exhibited significant (*p*

12

301 < 0.05) larger η values than other solvents, indicating that DMF had stronger dissolving

302 capacity for large organic molecules than MeOH.

303   Concentrations of extracted OC fractions in MeOH, MeOH/DCM mixtures, and

304 THF based on the two methods for rOC measurements (*section 2.2*) are compared in

305 Figures S1 and S2. The total SEOC concentrations derived from the two methods are

306 compared in Figure S3. All the scatter data of SEOC fell along the 1:1 line with

307 significant correlations ($r > 0.85$, $p < 0.01$). Because the measurement uncertainty of

308 dominant species is lower than minor ones (Hyslop and White, 2008; Yang et al., 2021),

309 the slightly greater relative difference between the two methods for extractable OC1

310 was likely attributed to its low concentrations (< 1 μg m^{-3}; Tables 1 and S1). Thus,

311 baking extracted filters to dryness was expected to have little influence on SEOC

312 measurements, particularly for low-volatility OC fractions (OC2-OC4).

313   Although water dissolves less OC than MeOH, WSOC is intensively extracted and

314 analyzed for its composition and light absorption (Hecobian et al., 2010; Liu et al., 2013;

315 Washenfelder et al., 2015). WSOC can play a significant role in changing the radiative

316 and cloud-nucleating properties of atmospheric aerosols (Hallar et al., 2013; Taylor et

317 al., 2017). It also served as a proxy measurement for oxygenated (OOA) or secondary

318 organic aerosols (SOA) in some regions (Kondo et al., 2007; Weber et al., 2007). In

319 previous work, MeOH was commonly used as the most efficient solvent in extracting

320 OC from biomass burning (η > 90%; Chen and Bond, 2010; Xie et al., 2017b) and

321 ambient particles (η ~80%; Xie et al., 2019b; Xie et al., 2022). MeOH-insoluble OC

322 has rarely been investigated through direct solvent-extraction followed by instrumental

323 analysis. There is evidence showing that BrC absorption is associated mostly with large

324 molecular weight and extremely low-volatility species (Saleh et al., 2014; Di Lorenzo

325 and Young, 2016; Di Lorenzo et al., 2017). Compared with DMF, the lower capability

of MeOH in dissolving OC3 and OC4 would lead to an underestimation of BrC absorption in atmospheric aerosols.

3.1.2 Light absorption of different solvent extracts

Table 2 shows the average Abs_λ and MAE_λ values of different solvent extracts at 365 and 550 nm. The Abs_λ and MAE_λ spectra of selected samples are illustrated in Figure S4. Not including DMF, MeOH extracts exhibited the strongest light absorption. Since MeOH can dissolve more OC3 and OC4 than DCM (Table 1), the Abs_λ and MAE_λ of MeOH/DCM extracts decreased as the fraction of DCM increased in solvent mixtures (Table 2 and Figure S4). Water and THF extracts had the smallest Abs_λ and MAE_λ due to their low extraction efficiencies for low-volatility OC (OC2-OC4; Table 1). In comparison to MeOH extracts, $Abs_{365/550}$ and $MAE_{365/550}$ of DMF extracts were at least more than 40% higher ($p < 0.05$). Given that the relative difference in extraction efficiency of total OC between MeOH and DMF was less than 10% and DMF dissolved more OC3 and OC4 than other solvents (Table 1), low-volatility OC should contain stronger light-absorbing chromophores (Saleh et al., 2014) and its mass fraction might determine the difference in BrC absorption across solvent extraction methods. Moreover, the relative difference in Abs_λ and MAE_λ between MeOH and DMF extracts increased with wavelength (Table 2 and Figure S4). This is because the light absorption of DMF extracts that contain stronger BrC chromophores depends less on wavelengths than other solvent extracts (Å ~4.5, Table 2). As shown in Figure S5, average Å and $MAE_{365/550}$ values of individual solvent extracts in Table 2 are negatively correlated.

In this work, insoluble organic particles coming off the filter during sonication might lead to overestimated SEOC concentrations and η values, and then the MAE_λ of solvent extracts would be underestimated. Previous studies rarely considered the loss of insoluble OC during the extraction process (Yan et al., 2020), of which the impact

351 on MAE$_\lambda$ calculation was still inconclusive. But Abs$_\lambda$ measurements would never be

352 influenced, as the light absorbance of solvent extracts was analyzed after filtration. In

353 Table 2, the second extraction only increases the average Abs$_{365}$ and Abs$_{550}$ values of

354 DMF extracts by 6.70% ($p = 0.78$) and 6.76% ($p = 0.77$), respectively. We suspected

355 that the difference in η values of DMF between one-time and two-time extraction

356 procedures was mainly ascribed to the detachment of insoluble OC particles.

357 In Figure S6, the absorbance spectra of 4-nitrophenol and 4-nitrocatechol in water

358 shift toward longer wavelengths compared to their MeOH solution. This is because

359 neutral and deprotonated forms of 4-nitrophenol and 4-nitrocatechol may have different

360 absorbance spectra, and these two compounds are deprotonated at pH $\approx$ 7 (Lin et al.,

361 2015b, 2017). The strong light absorption of 4-nitrophenol and 4-nitrocatechol in DMF

362 at 450 nm was not observed in other solvents, and was likely caused by unknown

363 reactions. Then the solvent effect introduced by DMF might overestimate the light

364 absorption of low-molecular-weight (LMW) nitrophenol-like species at > 400 nm in

365 source or ambient aerosols. Evidence shows that BrC absorption is dominated by large

366 molecules with extremely low volatility (Saleh et al., 2014; Di Lorenzo and Young,

367 2016; Di Lorenzo et al., 2017), and LMW nitrophenol-like species have very low

368 contributions to particulate OM (e.g., < 1%) and aerosol extract absorption (e.g., <10%)

369 (Mohr et al., 2013; Zhang et al., 2013; Teich et al., 2017; Xie et al., 2019a, 2020; Li et

370 al., 2020). The shapes of the light absorption spectra of aerosol extracts in DMF were

371 similar to other solvents (Figure S4) and PAH solutions (Figure S6g-l), and no elevation

372 in light absorption appeared at 400–500 nm. Thus, the overestimated absorption of

373 LMW nitrophenol-like species in DMF might not substantially impact the overall BrC

374 absorption of aerosol extracts. Furthermore, the absorbance of 4-nitrophenol and 4-

375 nitrocatechol in DMF at 365 nm (A$_{365}$) was lower than that in MeOH, and PAH

15

376 solutions showed very similar absorbance spectra across the five solvents (Figure S6g–

377 l and Table S5). Considering that low-volatility OC fractions (e.g., OC3 and OC4) in

378 the ambient are less water soluble (Table 1) and have a high degree of conjugation

379 (Chen and Bond, 2010; Lin et al., 2014), their structures are probably featured by a

380 PAH skeleton. Therefore, the large difference in Abs_{365} between DMF and MeOH

381 extracts (Table 2) was primarily ascribed to the fact that DMF can dissolve more OC3

382 and OC4 than methanol (Table 1). However, we cannot rule out the impact of solvent

383 effects on the comparison of light absorption spectra between MeOH and DMF extracts

384 (Figure S4), and more work is warranted in identifying the structures more soluble in

385 DMF than in MeOH.

386 *3.2 Collocated measurements and temporal variability*

387 Abs_{365} values of collocated Q_f and Q_b extracts in DMF are summarized in Table S6.

388 No significant difference was observed (Q_f $p = 0.96$; Q_b $p = 0.42$) between the two

389 samplers. After Q_b corrections, Abs_{365}, MAE_{365}, and Å of DMF extractable OC ($Abs_{365,d}$,

390 $MAE_{365,d}$, and $Å_d$) in $PM_{2.5}$ were calculated by averaging each pair of duplicate Q_f–Q_b

391 data, and are compared with those of methanol extracts ($Abs_{365,m}$, $MAE_{365,m}$, and $Å_m$)

392 in Table 3. Figure 1 shows comparisons between collocated measurements of $Abs_{365,d}$,

393 $MAE_{365,d}$, and $Å_d$. Generally, all comparisons indicated good agreement with COD <

394 0.20 (0.094–0.15). $Abs_{365,d}$ and $MAE_{365,d}$ had comparable uncertainty fractions (ARPD,

395 22.7% and 24.5%, Figure 1) as $Abs_{365,m}$ and $MAE_{365,m}$ (28.4% and 28.8%; Xie et al.,

396 2022). Since different primary combustion sources can have similar spectral

397 dependence for BrC absorption (Chen and Bond, 2010; Xie et al., 2017b; Xie et al.,

398 2018; Xie et al., 2019a), most $Å_d$ data clustered on the identity line with much lower

399 variability than $Abs_{365,d}$ and $MAE_{365,d}$. As shown in Table 3, average $Abs_{365,d}$ and

400 $MAE_{365,d}$ values were 30.7% ($p < 0.01$) and 17.3% ($p < 0.05$) larger than average

16

401 $Abs_{365,m}$ and $MAE_{365,m}$. Because the k value of BrC in bulk solution is directly estimated

402 from Abs_λ or MAE_λ (Liu et al., 2013; Liu et al., 2016; Lu et al., 2015), the estimation

403 method needs to be revised when ambient BrC is extracted using DMF instead of

404 MeOH. Both $MAE_{365,d}$ and $MAE_{365,m}$ were negatively correlated ($p < 0.01$) with their

405 corresponding Å values (Figure S7), and the lower average $Å_d$ (5.25 ± 0.64, $p < 0.01$)

406 compared to $Å_m$ (6.81± 1.64; Table 3) supports that more-absorbing BrC had less

407 spectral dependence than less-absorbing BrC.

408   Figure 2 compares the time series of Abs_{365}, MAE_{365}, and Å between the DMF and

409 MeOH extracts. Both DMF and MeOH extracts had significant ($p < 0.05$) higher

410 absorption at night-time than during the daytime due to the "photo-bleaching" effect

411 (Zhang et al., 2020; Xie et al., 2022). All the three parameters of DMF and MeOH

412 extracts exhibited consistency in winter (Figure 2) when biomass burning dominated

413 BrC absorption (Xie et al., 2022). While in later spring and summer (2019/05/15–

414 2019/08/01), average $Abs_{365,d}$ and $MAE_{365,d}$ values were more than two times greater

415 than the average $Abs_{365,m}$ and $MAE_{365,m}$. Many studies have identified a temporal

416 pattern of BrC absorption with winter maxima and summer minima based on

417 water/MeOH extraction methods (Lukács et al., 2007; Zhang et al., 2010; Du et al.,

418 2014; Zhu et al., 2018). Due to the low capability of water and MeOH in dissolving

419 large BrC molecules, BrC absorption and its temporal variations in these studies might

420 be biased. Moreover, the identification of BrC sources using receptor models is highly

421 dependent on the difference in the time series of input species (Dall'Osto et al., 2013).

422 Then, using DMF instead of MeOH for BrC extraction and measurements will lead to

423 distinct source apportionment results.

424 *3.3 Sources of DMF and MeOH Extractable BrC*

425   A final factor number of eight was determined based on the interpretability of

17

different base-case solutions (four to ten factors), the change in Q/Q_{exp} with factor numbers, and robustness analysis (Text S2 and Table S4). Normalized factor profiles of seven- to nine-factor solutions are compared in Figure S8. The seven-factor solution failed to resolve the lubricating oil combustion factor characterized by hopanes and steranes (Figure S8c). An unknown factor containing various source tracers related to crustal dust (Ca^{2+} and Mg^{2+}), lubricating oil (hopanes and steranes), and soil microbiota (sugar and sugar alcohols) was identified in the nine-factor solution (Figure S8i). Median and mean values of input $Abs_{365,d}$, $Abs_{365,m}$, and bulk component concentrations agreed well with PMF estimations (Table S7), and the strong correlations ($r = 0.86$– 0.99) between observations and PMF estimations indicated that the eight-factor solution simulated the time series of input species well. In comparison to Xie et al. (2022), where Abs_{365} of MeOH and water extracts were apportioned to nine sources using the same speciation data, this work lumped secondary nitrate and sulfate to the same factor (termed "secondary inorganics", Figure S8h), and the other seven factors had similar factor profiles linked with biomass burning, non-combustion fossil, lubricating oil combustion, coal combustion, dust resuspension, biogenic emission, and isoprene oxidation. Interpretations of individual factors based on characteristic source tracers and contribution time series were provided in previous work (Gou et al., 2021; Xie et al., 2022).

The average relative contributions of the identified factors to $Abs_{365,d}$, $Abs_{365,m}$, and bulk components are listed in Table S8. Consistent contribution distributions of $Abs_{365,m}$ were observed between Xie et al. (2022) and this study, indicating that the PMF results were robust to the inclusion of $Abs_{365,d}$ data. Figure 3 compares the time series of factor contributions to $Abs_{365,d}$ and $Abs_{365,m}$. ARPD and COD values between factor contributions to $Abs_{365,d}$ and $Abs_{365,m}$ and the absolute difference are exhibited in Figure

S9. $Abs_{365,d}$ and $Abs_{365,m}$ had comparable contributions from biomass burning, lubricating oil combustion, and coal combustion (Figure 3a, c, d). The small COD values of these three factors (0.0041–0.17) indicated no significant divergence. The biogenic emission and isoprene oxidation factors exhibited complete difference (ARPD = 200%, COD = 1; Figure S9f, g) as they had no contribution to $Abs_{365,m}$. Among the eight factors, the non-combustion fossil, dust resuspension, and isoprene oxidation factors had the largest median difference in factor contributions to $Abs_{365,d}$ and $Abs_{365,m}$ (0.63–0.67 Mm^{-1}) with substantial heterogeneity (COD > 0.20), followed by the secondary inorganics factor (0.20 Mm^{-1}, COD = 0.41). The temporal variations of the absolute difference shown in Figure S9 are identical to the contributions of individual factors to $Abs_{365,d}$ or $Abs_{365,m}$ (Figure 3).

The non-combustion fossil factor represents unburned fossil-fuel emissions (e.g., petroleum products), which contain substantial large organic molecules (e.g., high MW PAHs; Simoneit and Fetzer, 1996; Mi et al., 2000). This might explain why the non-combustion fossil factor contributed more $Abs_{365,d}$ than $Abs_{365,m}$ all over the year (Figure S9b). Dust resuspension and isoprene oxidation factors show prominent contributions to $Abs_{365,d}$ in spring and summer, respectively (Figure 3e, g). The dust resuspension factor had the highest average contributions to both crustal materials (Ca^{2+} and Mg^{2+}) and carbonaceous species (OC and EC; Table S8 and Figure S8), and was considered a mixed source of crustal dust and motor vehicle emissions (Yu et al., 2020; Xie et al., 2022). Besides the influences from primary emissions, aging processes of organic components in dust aerosols can induce the formation of BrC through iron-catalyzed polymerization (Link et al., 2020; Al-Abadleh, 2021; Chin et al., 2021). It was demonstrated that the isoprene-derived polymerization products through aerosol-phase reactions are light-absorbing chromophores (Lin et al., 2014; Nakayama et al.,

476 2015). This might explain the elevated difference between $Abs_{365,d}$ and $Abs_{365,m}$

477 contributions of the isoprene oxidation factor in summer (Figure S9g). The biogenic

478 emission factor was characterized by tracers related to microbiota activities (sugar and

479 sugar alcohols) and decomposition of high plant materials (odd-numbered alkanes) in

480 soil (Rogge et al., 1993; Simoneit et al., 2004), and had negligible contributions ($<0.1\%$)

481 to $Abs_{365,d}$ and $Abs_{365,m}$. Evidence shows that secondary BrC can be generated through

482 gas-phase reactions of anthropogenic volatile organic compounds with NO_X

483 (Nakayama et al., 2010; Liu et al., 2016; Xie et al., 2017a), aqueous reactions of SOA

484 with reduced nitrogen-containing species (e.g., NH_4^+; Updyke et al., 2012; Powelson et

485 al., 2014; Lin et al., 2015a), and evaporation of water from droplets in the atmosphere

486 containing soluble organics (Nguyen et al., 2012; Kasthuriarachchi et al., 2020). These

487 processes can also lead to the formation of low-volatility oligomers (Nguyen et al.,

488 2012; Song et al., 2013), and their contributions might be lumped into the secondary

489 inorganics factor due to the lack of OMMs. According to these results, one possible

490 explanation for the difference in time series between $Abs_{365,d}$ and $Abs_{365,m}$ (Figure 2) is

491 that large BrC molecules from unburned fossil fuels and atmospheric processes are less

492 soluble in MeOH than in DMF.

493 **4. Conclusions and implications**

494 Comparisons of extraction efficiencies and light absorption of ambient aerosol

495 extracts across selected solvents and solvent mixtures indicate that MeOH may

496 sometimes be replaced with DMF for measuring BrC absorption, as low-volatility OC

497 fractions containing strong chromophores are less soluble in MeOH than in DMF.

498 Existing modeling studies on the radiative forcing of BrC (Feng et al., 2013; Wang et

499 al., 2014; Zhang et al., 2020) often retrieved or estimated its optical properties from

500 laboratory or ambient measurements based on water/methanol extraction methods

(Chen and Bond, 2010; Hecobian et al., 2010; Liu et al., 2013; Zhang et al., 2013), and had a potential to underestimate the contribution of BrC to total aerosol absorption. However, the influence of the solvent effect was not accounted for in this work when comparing the light absorption of different solvent extracts. The difference between MeOH and DMF extract absorption might change with the time and location due to the variations in BrC sources. The results of this work also imply the necessity of applying different solvents or combinations of solvents with broad polarity and dissolving capability to study BrC composition and absorption, particularly for low-volatility fractions.

Although light-absorbing properties of DMF and MeOH extracts had good agreement in cold periods, when biomass and coal burning sources dominated BrC emissions, their distinct time series in spring and summer implies that the contributions of certain BrC sources were underestimated or missed when the MeOH extraction method was used. Source apportionment results of $Abs_{365,d}$ and $Abs_{365,m}$ based on organic molecular marker data indicated that large and methanol insoluble BrC molecules are likely coming from unburned fossil fuels and polymerization of aerosol organics. Laboratory studies have observed the polymerization process through heterogeneous reactions of several precursors (e.g., catechol; Lin et al., 2014; Link et al., 2020), but the structures and light-absorbing properties of potential polymerization products in ambient aerosols (Figure 3e, g) are less understood and warrant further study.

Data availability

Data used in the writing of this paper is available at the Harvard Dataverse (https://doi.org/10.7910/DVN/CGHPXB, Xu et al., 2022)

References

540 Al-Abadleh, H. A.: Aging of atmospheric aerosols and the role of iron in catalyzing brown carbon
541   formation, Environ. Sci.: Atmos., 1, 297-345, 10.1039/D1EA00038A, 2021.
542 Atwi, K., Cheng, Z., El Hajj, O., Perrie, C., and Saleh, R.: A dominant contribution to light absorption
543   by methanol-insoluble brown carbon produced in the combustion of biomass fuels typically
544   consumed in wildland fires in the United States, Environ. Sci.: Atmos., 10.1039/D1EA00065A, 2022.
545 Bai, Z., Zhang, L., Cheng, Y., Zhang, W., Mao, J., Chen, H., Li, L., Wang, L., and Chen, J.:
546   Water/methanol-insoluble brown carbon can dominate aerosol-enhanced light absorption in port
547   cities, Environ. Sci. Technol., 54, 14889-14898, 10.1021/acs.est.0c03844, 2020.
548 Chen, Y., and Bond, T. C.: Light absorption by organic carbon from wood combustion, Atmos. Chem.
549   Phys., 10, 1773-1787, 10.5194/acp-10-1773-2010, 2010.
550 Cheng, Z., Atwi, K., Hajj, O. E., Ijeli, I., Fischer, D. A., Smith, G., and Saleh, R.: Discrepancies between
551   brown carbon light-absorption properties retrieved from online and offline measurements, Aerosol
552   Sci. Technol., 55, 92-103, 10.1080/02786826.2020.1820940, 2021.
553 Chin, H., Hopstock, K. S., Fleming, L. T., Nizkorodov, S. A., and Al-Abadleh, H. A.: Effect of aromatic
554   ring substituents on the ability of catechol to produce brown carbon in iron(iii)-catalyzed reactions,
555   Environ. Sci.: Atmos., 1, 64-78, 10.1039/D0EA00007H, 2021.
556 Dall'Osto, M., Querol, X., Amato, F., Karanasiou, A., Lucarelli, F., Nava, S., Calzolai, G., and Chiari,
557   M.: Hourly elemental concentrations in PM2.5 aerosols sampled simultaneously at urban
558   background and road site during SAPUSS – diurnal variations and PMF receptor modelling, Atmos.
559   Chem. Phys., 13, 4375-4392, 10.5194/acp-13-4375-2013, 2013.
560 Di Lorenzo, R. A., and Young, C. J.: Size separation method for absorption characterization in brown
561   carbon: Application to an aged biomass burning sample, Geophys. Res. Lett., 43, 458-465,
562   10.1002/2015gl066954, 2016.
563 Di Lorenzo, R. A., Washenfelder, R. A., Attwood, A. R., Guo, H., Xu, L., Ng, N. L., Weber, R. J.,
564   Baumann, K., Edgerton, E., and Young, C. J.: Molecular-size-separated brown carbon absorption for

biomass-burning aerosol at multiple field sites, Environ. Sci. Technol., 51, 3128-3137, 10.1021/acs.est.6b06160, 2017.

Du, Z., He, K., Cheng, Y., Duan, F., Ma, Y., Liu, J., Zhang, X., Zheng, M., and Weber, R.: A yearlong study of water-soluble organic carbon in Beijing I: Sources and its primary vs. secondary nature, Atmos. Environ., 92, 514-521, https://doi.org/10.1016/j.atmosenv.2014.04.060, 2014.

Feng, Y., Ramanathan, V., and Kotamarthi, V. R.: Brown carbon: a significant atmospheric absorber of solar radiation? Atmos. Chem. Phys., 13, 8607-8621, 10.5194/acp-13-8607-2013, 2013.

Gou, Y., Qin, C., Liao, H., and Xie, M.: Measurements, gas/particle partitioning, and sources of nonpolar organic molecular markers at a suburban site in the west Yangtze River Delta, China, J. Geophys. Res. Atmos., 126, e2020JD034080, https://doi.org/10.1029/2020JD034080, 2021.

Hallar, A. G., Lowenthal, D. H., Clegg, S. L., Samburova, V., Taylor, N., Mazzoleni, L. R., Zielinska, B. K., Kristensen, T. B., Chirokova, G., McCubbin, I. B., Dodson, C., and Collins, D.: Chemical and hygroscopic properties of aerosol organics at Storm Peak Laboratory, J. Geophys. Res. Atmos., 118, 4767-4779, https://doi.org/10.1002/jgrd.50373, 2013.

Hecobian, A., Zhang, X., Zheng, M., Frank, N., Edgerton, E. S., and Weber, R. J.: Water-Soluble Organic Aerosol material and the light-absorption characteristics of aqueous extracts measured over the Southeastern United States, Atmos. Chem. Phys., 10, 5965-5977, 10.5194/acp-10-5965-2010, 2010.

Hems, R. F., Schnitzler, E. G., Liu-Kang, C., Cappa, C. D., and Abbatt, J. P. D.: Aging of atmospheric brown carbon aerosol, ACS Earth Space Chem., 5, 722-748, 10.1021/acsearthspacechem.0c00346, 2021.

Huang, R.-J., Yang, L., Cao, J., Chen, Y., Chen, Q., Li, Y., Duan, J., Zhu, C., Dai, W., Wang, K., Lin, C., Ni, H., Corbin, J. C., Wu, Y., Zhang, R., Tie, X., Hoffmann, T., O'Dowd, C., and Dusek, U.: Brown carbon aerosol in urban Xi'an, northwest China: The composition and light absorption properties, Environ. Sci. Technol., 52, 6825-6833, 10.1021/acs.est.8b02386, 2018.

Huang, R.-J., Yang, L., Shen, J., Yuan, W., Gong, Y., Guo, J., Cao, W., Duan, J., Ni, H., Zhu, C., Dai, W., Li, Y., Chen, Y., Chen, Q., Wu, Y., Zhang, R., Dusek, U., O'Dowd, C., and Hoffmann, T.: Water-insoluble organics dominate brown carbon in wintertime urban aerosol of China: Chemical characteristics and optical properties, Environ. Sci. Technol., 54, 7836-7847, 10.1021/acs.est.0c01149, 2020.

Hyslop, N. P., and White, W. H.: An evaluation of interagency monitoring of protected visual environments (IMPROVE) collocated precision and uncertainty estimates, Atmos. Environ., 42, 2691-2705, https://doi.org/10.1016/j.atmosenv.2007.06.053, 2008.

Kasthuriarachchi, N. Y., Rivellini, L.-H., Chen, X., Li, Y. J., and Lee, A. K. Y.: Effect of relative humidity on secondary brown carbon formation in aqueous droplets, Environ. Sci. Technol., 54, 13207-13216, 10.1021/acs.est.0c01239, 2020.

Kondo, Y., Miyazaki, Y., Takegawa, N., Miyakawa, T., Weber, R. J., Jimenez, J. L., Zhang, Q., and Worsnop, D. R.: Oxygenated and water-soluble organic aerosols in Tokyo, J. Geophys. Res. Atmos., 112, D01203, 10.1029/2006jd007056, 2007.

Lack, D. A., Langridge, J. M., Bahreini, R., Cappa, C. D., Middlebrook, A. M., and Schwarz, J. P.: Brown carbon and internal mixing in biomass burning particles, Proc. Natl. Acad. Sci. U.S.A., 109, 14802-14807, 10.1073/pnas.1206575109, 2012.

Laskin, A., Laskin, J., and Nizkorodov, S. A.: Chemistry of atmospheric brown carbon, Chem. Rev., 115, 4335-4382, 10.1021/cr5006167, 2015.

Li, X., Yang, Y., Liu, S., Zhao, Q., Wang, G., and Wang, Y.: Light absorption properties of brown carbon (BrC) in autumn and winter in Beijing: Composition, formation and contribution of nitrated aromatic compounds, Atmos. Environ., 223, 117289, https://doi.org/10.1016/j.atmosenv.2020.117289, 2020.

Li, Y., Ji, Y., Zhao, J., Wang, Y., Shi, Q., Peng, J., Wang, Y., Wang, C., Zhang, F., Wang, Y., Seinfeld, J. H., and Zhang, R.: Unexpected oligomerization of small α-dicarbonyls for secondary organic aerosol and brown carbon formation, Environ. Sci. Technol., 55, 4430-4439, 10.1021/acs.est.0c08066, 2021.

Lin, P., Laskin, J., Nizkorodov, S. A., and Laskin, A.: Revealing brown carbon chromophores produced in reactions of methylglyoxal with ammonium sulfate, Environ. Sci. Technol., 49, 14257-14266, 10.1021/acs.est.5b03608, 2015a

Lin, P., Liu, J. M., Shilling, J. E., Kathmann, S. M., Laskin, J., and Laskin, A.: Molecular characterization of brown carbon (BrC) chromophores in secondary organic aerosol generated from photo-oxidation of toluene, Phys. Chem. Chem. Phys., 17, 23312-23325, 10.1039/c5cp02563j, 2015b.

Lin, P., Bluvshtein, N., Rudich, Y., Nizkorodov, S. A., Laskin, J., and Laskin, A.: Molecular chemistry of atmospheric brown carbon inferred from a nationwide biomass burning event, Environ. Sci. Technol., 51, 11561-11570, 10.1021/acs.est.7b02276, 2017.

Lin, P., Aiona, P. K., Li, Y., Shiraiwa, M., Laskin, J., Nizkorodov, S. A., and Laskin, A.: Molecular

characterization of brown carbon in biomass burning aerosol particles, Environ. Sci. Technol., 50, 11815-11824, 10.1021/acs.est.6b03024, 2016.

Lin, Y.-H., Budisulistiorini, S. H., Chu, K., Siejack, R. A., Zhang, H., Riva, M., Zhang, Z., Gold, A., Kautzman, K. E., and Surratt, J. D.: Light-absorbing oligomer formation in secondary organic aerosol from reactive uptake of isoprene epoxydiols, Environ. Sci. Technol., 48, 12012-12021, 10.1021/es503142b, 2014.

Link, N., Removski, N., Yun, J., Fleming, L. T., Nizkorodov, S. A., Bertram, A. K., and Al-Abadleh, H. A.: Dust-catalyzed oxidative polymerization of catechol and its impacts on ice nucleation efficiency and optical properties, ACS Earth Space Chem., 4, 1127-1139, 10.1021/acsearthspacechem.0c00107, 2020.

Liu, J., Bergin, M., Guo, H., King, L., Kotra, N., Edgerton, E., and Weber, R. J.: Size-resolved measurements of brown carbon in water and methanol extracts and estimates of their contribution to ambient fine-particle light absorption, Atmos. Chem. Phys., 13, 12389-12404, 10.5194/acp-13-12389-2013, 2013.

Liu, J., Lin, P., Laskin, A., Laskin, J., Kathmann, S. M., Wise, M., Caylor, R., Imholt, F., Selimovic, V., and Shilling, J. E.: Optical properties and aging of light-absorbing secondary organic aerosol, Atmos. Chem. Phys., 16, 12815-12827, 10.5194/acp-16-12815-2016, 2016.

Lu, Z., Streets, D. G., Winijkul, E., Yan, F., Chen, Y., Bond, T. C., Feng, Y., Dubey, M. K., Liu, S., Pinto, J. P., and Carmichael, G. R.: Light absorption properties and radiative effects of primary organic aerosol emissions, Environ. Sci. Technol., 49, 4868-4877, 10.1021/acs.est.5b00211, 2015.

Lukács, H., Gelencsér, A., Hammer, S., Puxbaum, H., Pio, C., Legrand, M., Kasper-Giebl, A., Handler, M., Limbeck, A., Simpson, D., and Preunkert, S.: Seasonal trends and possible sources of brown carbon based on 2-year aerosol measurements at six sites in Europe, J. Geophys. Res. Atmos., 112, https://doi.org/10.1029/2006JD008151, 2007.

Mack, L. A., Levin, E. J. T., Kreidenweis, S. M., Obrist, D., Moosmüller, H., Lewis, K. A., Arnott, W. P., McMeeking, G. R., Sullivan, A. P., Wold, C. E., Hao, W. M., Collett Jr, J. L., and Malm, W. C.: Optical closure experiments for biomass smoke aerosols, Atmos. Chem. Phys., 10, 9017-9026, 10.5194/acp-10-9017-2010, 2010.

Mo, Y., Li, J., Liu, J., Zhong, G., Cheng, Z., Tian, C., Chen, Y., and Zhang, G.: The influence of solvent and pH on determination of the light absorption properties of water-soluble brown carbon, Atmos. Environ., 161, 90-98, https://doi.org/10.1016/j.atmosenv.2017.04.037, 2017.

Mohr, C., Lopez-Hilfiker, F. D., Zotter, P., Prévôt, A. S. H., Xu, L., Ng, N. L., Herndon, S. C., Williams, L. R., Franklin, J. P., Zahniser, M. S., Worsnop, D. R., Knighton, W. B., Aiken, A. C., Gorkowski, K. J., Dubey, M. K., Allan, J. D., and Thornton, J. A.: Contribution of nitrated phenols to wood burning brown carbon light absorption in Detling, United Kingdom during winter time, Environ. Sci. Technol., 47, 6316-6324, 10.1021/es400683v, 2013.

Moschos, V., Gysel-Beer, M., Modini, R. L., Corbin, J. C., Massabò, D., Costa, C., Danelli, S. G., Vlachou, A., Daellenbach, K. R., Szidat, S., Prati, P., Prévôt, A. S. H., Baltensperger, U., and El Haddad, I.: Source-specific light absorption by carbonaceous components in the complex aerosol matrix from yearly filter-based measurements, Atmos. Chem. Phys., 21, 12809-12833, 10.5194/acp-21-12809-2021, 2021.

Mi, H.-H., Lee, W.-J., Chen, C.-B., Yang, H.-H., and Wu, S.-J.: Effect of fuel aromatic content on PAH emission from a heavy-duty diesel engine, Chemosphere, 41, 1783-1790, https://doi.org/10.1016/S0045-6535(00)00043-6, 2000.

Nakayama, T., Matsumi, Y., Sato, K., Imamura, T., Yamazaki, A., and Uchiyama, A.: Laboratory studies on optical properties of secondary organic aerosols generated during the photooxidation of toluene and the ozonolysis of α-pinene, J. Geophys. Res. Atmos., 115, D24204, 10.1029/2010jd014387, 2010.

Nakayama, T., Sato, K., Tsuge, M., Imamura, T., and Matsumi, Y.: Complex refractive index of secondary organic aerosol generated from isoprene/NOx photooxidation in the presence and absence of SO2, J. Geophys. Res. Atmos., 120, 7777-7787, https://doi.org/10.1002/2015JD023522, 2015.

Nguyen, T. B., Lee, P. B., Updyke, K. M., Bones, D. L., Laskin, J., Laskin, A., and Nizkorodov, S. A.: Formation of nitrogen- and sulfur-containing light-absorbing compounds accelerated by evaporation of water from secondary organic aerosols, J. Geophys. Res. Atmos., 117, D01207, 10.1029/2011jd016944, 2012.

Powelson, M. H., Espelien, B. M., Hawkins, L. N., Galloway, M. M., and De Haan, D. O.: Brown carbon formation by aqueous-phase carbonyl compound reactions with amines and ammonium sulfate, Environ. Sci. Technol., 48, 985-993, 10.1021/es4038325, 2014.

Qin, C., Gou, Y., Wang, Y., Mao, Y., Liao, H., Wang, Q., and Xie, M.: Gas–particle partitioning of polyol

683   tracers at a suburban site in Nanjing, east China: increased partitioning to the particle phase, Atmos.
684   Chem. Phys., 21, 12141-12153, 10.5194/acp-21-12141-2021, 2021.
685 Rogge, W. F., Hildemann, L. M., Mazurek, M. A., Cass, G. R., and Simoneit, B. R. T.: Sources of fine
686   organic aerosol .4. Particulate abrasion products from leaf surfaces of urban plants, Environ. Sci.
687   Technol., 27, 2700-2711, 10.1021/es00049a008, 1993.
688 Saleh, R., Hennigan, C. J., McMeeking, G. R., Chuang, W. K., Robinson, E. S., Coe, H., Donahue, N.
689   M., and Robinson, A. L.: Absorptivity of brown carbon in fresh and photo-chemically aged biomass-
690   burning emissions, Atmos. Chem. Phys., 13, 7683-7693, 10.5194/acp-13-7683-2013, 2013.
691 Saleh, R., Robinson, E. S., Tkacik, D. S., Ahern, A. T., Liu, S., Aiken, A. C., Sullivan, R. C., Presto, A.
692   A., Dubey, M. K., Yokelson, R. J., Donahue, N. M., and Robinson, A. L.: Brownness of organics in
693   aerosols from biomass burning linked to their black carbon content, Nat. Geosci., 7, 647-650,
694   https://doi.org/10.1038/ngeo2220, 2014.
695 Saleh, R.: From measurements to models: Toward accurate representation of brown carbon in climate
696   calculations, Curr. Pollut. Rep., 6, 90-104, 10.1007/s40726-020-00139-3, 2020.
697 Schauer, J. J., Mader, B. T., Deminter, J. T., Heidemann, G., Bae, M. S., Seinfeld, J. H., Flagan, R. C.,
698   Cary, R. A., Smith, D., Huebert, B. J., Bertram, T., Howell, S., Kline, J. T., Quinn, P., Bates, T.,
699   Turpin, B., Lim, H. J., Yu, J. Z., Yang, H., and Keywood, M. D.: ACE-Asia intercomparison of a
700   thermal-optical method for the determination of particle-phase organic and elemental carbon,
701   Environ. Sci. Technol., 37, 993-1001, 10.1021/es020622f, 2003.
702 Shetty, N. J., Pandey, A., Baker, S., Hao, W. M., and Chakrabarty, R. K.: Measuring light absorption by
703   freshly emitted organic aerosols: Optical artifacts in traditional solvent-extraction-based methods,
704   Atmos. Chem. Phys., 19, 8817-8830, 10.5194/acp-19-8817-2019, 2019.
705 Simoneit, B. R. T., and Fetzer, J. C.: High molecular weight polycyclic aromatic hydrocarbons in
706   hydrothermal petroleums from the Gulf of California and Northeast Pacific Ocean, Org. Geochem.,
707   24, 1065-1077, https://doi.org/10.1016/S0146-6380(96)00081-2, 1996.
708 Simoneit, B. R. T., Elias, V. O., Kobayashi, M., Kawamura, K., Rushdi, A. I., Medeiros, P. M., Rogge,
709   W. F., and Didyk, B. M.: Sugars dominant water-soluble organic compounds in soils and
710   characterization as tracers in atmospheric particulate matter, Environ. Sci. Technol., 38, 5939-5949,
711   10.1021/es0403099, 2004.
712 Song, C., Gyawali, M., Zaveri, R. A., Shilling, J. E., and Arnott, W. P.: Light absorption by secondary
713   organic aerosol from α-pinene: Effects of oxidants, seed aerosol acidity, and relative humidity, J.
714   Geophys. Res. Atmos., 118, 11,741-711,749, 10.1002/jgrd.50767, 2013.
715 Taylor, N. F., Collins, D. R., Lowenthal, D. H., McCubbin, I. B., Hallar, A. G., Samburova, V., Zielinska,
716   B., Kumar, N., and Mazzoleni, L. R.: Hygroscopic growth of water soluble organic carbon isolated
717   from atmospheric aerosol collected at US national parks and Storm Peak Laboratory, Atmos. Chem.
718   Phys., 17, 2555-2571, 10.5194/acp-17-2555-2017, 2017.
719 Teich, M., van Pinxteren, D., Wang, M., Kecorius, S., Wang, Z., Müller, T., Močnik, G., and Herrmann,
720   H.: Contributions of nitrated aromatic compounds to the light absorption of water-soluble and
721   particulate brown carbon in different atmospheric environments in Germany and China, Atmos.
722   Chem. Phys., 17, 1653-1672, 10.5194/acp-17-1653-2017, 2017.
723 Updyke, K. M., Nguyen, T. B., and Nizkorodov, S. A.: Formation of brown carbon via reactions of
724   ammonia with secondary organic aerosols from biogenic and anthropogenic precursors, Atmos.
725   Environ., 63, 22-31, https://doi.org/10.1016/j.atmosenv.2012.09.012, 2012.
726 Wang, X., Heald, C. L., Ridley, D. A., Schwarz, J. P., Spackman, J. R., Perring, A. E., Coe, H., Liu, D.,
727   and Clarke, A. D.: Exploiting simultaneous observational constraints on mass and absorption to
728   estimate the global direct radiative forcing of black carbon and brown carbon, Atmos. Chem. Phys.,
729   14, 10989-11010, 10.5194/acp-14-10989-2014, 2014.
730 Wang, X., Heald, C. L., Liu, J., Weber, R. J., Campuzano-Jost, P., Jimenez, J. L., Schwarz, J. P., and
731   Perring, A. E.: Exploring the observational constraints on the simulation of brown carbon, Atmos.
732   Chem. Phys., 18, 635-653, 10.5194/acp-18-635-2018, 2018.
733 Wang, Y., Hu, M., Wang, Y., Zheng, J., Shang, D., Yang, Y., Liu, Y., Li, X., Tang, R., Zhu, W., Du, Z.,
734   Wu, Y., Guo, S., Wu, Z., Lou, S., Hallquist, M., and Yu, J. Z.: The formation of nitro-aromatic
735   compounds under high NOx and anthropogenic VOC conditions in urban Beijing, China, Atmos.
736   Chem. Phys., 19, 7649-7665, 10.5194/acp-19-7649-2019, 2019.
737 Washenfelder, R. A., Attwood, A. R., Brock, C. A., Guo, H., Xu, L., Weber, R. J., Ng, N. L., Allen, H.
738   M., Ayres, B. R., Baumann, K., Cohen, R. C., Draper, D. C., Duffey, K. C., Edgerton, E., Fry, J. L.,
739   Hu, W. W., Jimenez, J. L., Palm, B. B., Romer, P., Stone, E. A., Wooldridge, P. J., and Brown, S. S.:
740   Biomass burning dominates brown carbon absorption in the rural southeastern United States,
741   Geophys. Res. Lett., 42, 653-664, 10.1002/2014gl062444, 2015.

Weber, R. J., Sullivan, A. P., Peltier, R. E., Russell, A., Yan, B., Zheng, M., de Gouw, J., Warneke, C., Brock, C., Holloway, J. S., Atlas, E. L., and Edgerton, E.: A study of secondary organic aerosol formation in the anthropogenic-influenced southeastern United States, J. Geophys. Res. Atmos., 112, D13302, 10.1029/2007jd008408, 2007.

Xie, M., Chen, X., Hays, M. D., Lewandowski, M., Offenberg, J., Kleindienst, T. E., and Holder, A. L.: Light absorption of secondary organic aerosol: Composition and contribution of nitroaromatic compounds, Environ. Sci. Technol., 51, 11607-11616, 10.1021/acs.est.7b03263, 2017a.

Xie, M., Hays, M. D., and Holder, A. L.: Light-absorbing organic carbon from prescribed and laboratory biomass burning and gasoline vehicle emissions, Sci. Rep., 7, 7318, 10.1038/s41598-017-06981-8, 2017b.

Xie, M., Shen, G., Holder, A. L., Hays, M. D., and Jetter, J. J.: Light absorption of organic carbon emitted from burning wood, charcoal, and kerosene in household cookstoves, Environ. Pollut., 240, 60-67, https://doi.org/10.1016/j.envpol.2018.04.085, 2018.

Xie, M., Chen, X., Hays, M. D., and Holder, A. L.: Composition and light absorption of N-containing aromatic compounds in organic aerosols from laboratory biomass burning, Atmos. Chem. Phys., 19, 2899-2915, 10.5194/acp-19-2899-2019, 2019a.

Xie, M., Chen, X., Holder, A. L., Hays, M. D., Lewandowski, M., Offenberg, J. H., Kleindienst, T. E., Jaoui, M., and Hannigan, M. P.: Light absorption of organic carbon and its sources at a southeastern U.S. location in summer, Environ. Pollut., 244, 38-46, https://doi.org/10.1016/j.envpol.2018.09.125, 2019b.

Xie, M., Zhao, Z., Holder, A. L., Hays, M. D., Chen, X., Shen, G., Jetter, J. J., Champion, W. M., and Wang, Q.: Chemical composition, structures, and light absorption of N-containing aromatic compounds emitted from burning wood and charcoal in household cookstoves, Atmos. Chem. Phys., 20, 14077-14090, 10.5194/acp-20-14077-2020, 2020.

Xie, M., Peng, X., Shang, Y., Yang, L., Zhang, Y., Wang, Y., and Liao, H.: Collocated measurements of Light-absorbing organic carbon in PM2.5: Observation uncertainty and organic tracer-based source apportionment, J. Geophys. Res. Atmos., 127, e2021JD035874, https://doi.org/10.1029/2021JD035874, 2022.

Xu, Z., Feng, W., Wang, Y., Ye, H., Wang, Y., Liao, H., and Xie, M.: Replication Data for: Underestimation of brown carbon absorption based on the methanol extraction method and its impacts on source analysis, Harvard Dataverse, V2, https://doi.org/10.7910/DVN/CGHPXB, 2022.

Xu, L., Peng, Y., Ram, K., Zhang, Y., Bao, M., and Wei, J.: Investigation of the uncertainties of simulated optical properties of brown carbon at two Asian sites using a modified bulk aerosol optical scheme of the community atmospheric model version 5.3, J. Geophys. Res. Atmos., 126, e2020JD033942, https://doi.org/10.1029/2020JD033942, 2021.

Yan, F., Kang, S., Sillanpää, M., Hu, Z., Gao, S., Chen, P., Gautam, S., Reinikainen, S.-P., and Li, C.: A new method for extraction of methanol-soluble brown carbon: Implications for investigation of its light absorption ability, Environ. Pollut., 262, 114300, https://doi.org/10.1016/j.envpol.2020.114300, 2020.

Yang, L., Shang, Y., Hannigan, M. P., Zhu, R., Wang, Q. g., Qin, C., and Xie, M.: Collocated speciation of PM2.5 using tandem quartz filters in northern nanjing, China: Sampling artifacts and measurement uncertainty, Atmos. Environ., 246, 118066, https://doi.org/10.1016/j.atmosenv.2020.118066, 2021.

Yu, Y., Ding, F., Mu, Y., Xie, M., and Wang, Q. g.: High time-resolved PM2.5 composition and sources at an urban site in Yangtze River Delta, China after the implementation of the APPCAP, Chemosphere, 261, 127746, https://doi.org/10.1016/j.chemosphere.2020.127746, 2020.

Zhang, A., Wang, Y., Zhang, Y., Weber, R. J., Song, Y., Ke, Z., and Zou, Y.: Modeling the global radiative effect of brown carbon: a potentially larger heating source in the tropical free troposphere than black carbon, Atmos. Chem. Phys., 20, 1901-1920, 10.5194/acp-20-1901-2020, 2020.

Zhang, X., Hecobian, A., Zheng, M., Frank, N. H., and Weber, R. J.: Biomass burning impact on PM2.5 over the southeastern US during 2007: integrating chemically speciated FRM filter measurements, MODIS fire counts and PMF analysis, Atmos. Chem. Phys., 10, 6839-6853, 10.5194/acp-10-6839-2010, 2010.

Zhang, X., Lin, Y.-H., Surratt, J. D., and Weber, R. J.: Sources, composition and absorption Ångström exponent of light-absorbing organic components in aerosol extracts from the Los Angeles basin, Environ. Sci. Technol., 47, 3685-3693, 10.1021/es305047b, 2013.

Zhu, C.-S., Cao, J.-J., Huang, R.-J., Shen, Z.-X., Wang, Q.-Y., and Zhang, N.-N.: Light absorption properties of brown carbon over the southeastern Tibetan Plateau, Sci. Total Environ., 625, 246-251, https://doi.org/10.1016/j.scitotenv.2017.12.183, 2018.

Table 1. SEOC concentrations and extraction efficiencies (η, %) of total OC and OC fractions for different solvents.

	OC prior to extractions	Water[a]	MeOH[b]	MeOH/DCM (1:1)[b]	MeOH/DCM (1:2)[b]	THF[b]	DMF[a]
One-time extraction (N = 11)							
SEOC, $\mu g\ m^{-3}$							
Total OC	9.36 ± 2.27	6.38 ± 2.03	7.85 ± 2.40	7.08 ± 1.32	6.99 ± 1.71	6.14 ± 2.01	8.49 ± 2.52
OC1	0.66 ± 0.21	0.61 ± 0.20	0.64 ± 0.21	0.65 ± 0.20	0.64 ± 0.22	0.59 ± 0.18	0.59 ± 0.24
OC2	2.69 ± 0.55	2.20 ± 0.60	2.50 ± 0.55	2.34 ± 0.41	2.37 ± 0.46	2.09 ± 0.55	2.48 ± 0.60
OC3	3.35 ± 0.93	1.82 ± 0.80	2.48 ± 0.96	2.23 ± 0.49	2.18 ± 0.70	1.98 ± 0.93	2.86 ± 1.01
OC4	2.75 ± 0.81	1.76 ± 0.65	2.23 ± 0.84	1.86 ± 0.51	1.78 ± 0.61	1.48 ± 0.61	2.56 ± 0.87
η (%)							
Total OC		66.7 ± 8.58	82.3 ± 8.68	76.0 ± 7.70	74.3 ± 7.83	64.2 ± 8.08	89.0 ± 7.96
OC1		91.7 ± 4.85	96.1 ± 6.73	97.9 ± 5.02	97.4 ± 4.35	89.6 ± 9.55	88.8 ± 4.98
OC2		80.8 ± 8.11	92.7 ± 3.69	87.7 ± 5.87	88.5 ± 7.21	76.9 ± 7.62	91.4 ± 6.17
OC3		52.4 ± 11.8	73.0 ± 11.5	68.1 ± 8.64	65.2 ± 10.2	57.6 ± 12.0	84.3 ± 9.79
OC4		63.3 ± 9.13	80.3 ± 11.4	69.0 ± 9.26	64.5 ± 8.11	52.7 ± 5.86	92.8 ± 9.69
Two-time extraction (N = 10)							
SEOC, $\mu g\ m^{-3}$							
Total OC	10.9 ± 4.93	7.74 ± 4.01	9.33 ± 4.11	9.34 ± 4.19	9.11 ± 4.04	7.56 ± 3.38	10.4 ± 4.80
OC1	0.66 ± 0.47	0.62 ± 0.45	0.62 ± 0.49	0.59 ± 0.50	0.60 ± 0.51	0.59 ± 0.49	0.60 ± 0.47
OC2	2.76 ± 0.77	2.20 ± 0.59	2.60 ± 0.66	2.57 ± 0.65	2.60 ± 0.68	2.28 ± 0.53	2.69 ± 0.78
OC3	4.11 ± 2.01	2.55 ± 1.62	3.26 ± 1.62	3.37 ± 1.68	3.20 ± 1.58	2.62 ± 1.39	3.88 ± 1.95
OC4	3.36 ± 1.77	2.38 ± 1.42	2.84 ± 1.42	2.81 ± 1.47	2.71 ± 1.39	2.08 ± 1.06	3.23 ± 1.70
η (%)							
Total OC		69.9 ± 5.88	86.6 ± 7.86	86.2 ± 8.73	84.8 ± 7.76	70.1 ± 8.01	95.6 ± 3.67
OC1		93.6 ± 4.08	90.3 ± 13.9	82.6 ± 25.9	83.8 ± 22.4	82.9 ± 15.1	92.2 ± 13.9
OC2		80.1 ± 5.01	94.8 ± 4.20	93.6 ± 4.94	94.7 ± 2.51	83.5 ± 6.86	97.2 ± 2.12
OC3		59.0 ± 10.6	80.0 ± 10.2	82.3 ± 9.86	79.1 ± 10.6	63.9 ± 10.7	94.2 ± 4.15
OC4		69.3 ± 6.46	86.3 ± 12.0	84.3 ± 12.0	82.7 ± 13.3	62.9 ± 7.76	96.9 ± 5.18

[a] Concentrations of rOC in extracted filters were measured after the baking process (100 °C, 2 h); [b] rOC was measured when extracted filters were air dried.

Table 2. Light-absorbing properties of SEOC following one-time and two-time extraction procedures.

Solvent	Water	MeOH	MeOH/DCM (1:1)	MeOH/DCM (1:2)	THF	DMF
One-time extraction						
Abs_{365}, Mm^{-1}	5.13 ± 2.04	11.9 ± 5.83	10.3 ± 4.42	8.12 ± 3.38	5.48 ± 3.01	17.5 ± 8.05
Abs_{550}, Mm^{-1}	0.35 ± 0.12	1.28 ± 0.87	0.97 ± 0.55	0.35 ± 0.47	0.42 ± 0.47	4.40 ± 2.34
MAE_{365}, $m^2\,g^{-1}$ C	0.87 ± 0.19	1.46 ± 0.41	1.41 ± 0.36	1.13 ± 0.22	0.87 ± 0.25	2.02 ± 0.58
MAE_{550}, $m^2\,g^{-1}$ C	0.062 ± 0.028	0.15 ± 0.084	0.13 ± 0.054	0.042 ± 0.52	0.059 ± 0.56	0.30 ± 0.12
Å	6.63 ± 0.49	5.44 ± 0.75	5.65 ± 0.54	6.59 ± 0.66	6.17 ± 0.69	4.52 ± 0.41
Two-time extraction						
$Abs_{365,1st}$,[a] Mm^{-1}	6.64 ± 4.25	14.1 ± 7.09	14.6 ± 8.05	11.6 ± 6.78	7.17 ± 4.26	20.5 ± 10.6
$Abs_{550,1st}$,[a] Mm^{-1}	0.42 ± 0.12	1.34 ± 0.70	1.34 ± 0.83	0.84 ± 0.50	0.53 ± 0.27	2.82 ± 1.44
Abs_{365},[b] Mm^{-1}	8.26 ± 5.21	15.5 ± 7.76	16.8 ± 8.82	14.0 ± 8.91	8.35 ± 4.81	21.9 ± 11.2
Abs_{550},[b] Mm^{-1}	0.50 ± 0.18	1.60 ± 0.78	1.64 ± 0.99	1.22 ± 0.98	0.69 ± 0.43	3.01 ± 1.49
MAE_{365}, $m^2\,g^{-1}$ C	1.19 ± 0.26	1.70 ± 0.60	1.80 ± 0.52	1.50 ± 0.51	1.10 ± 0.40	2.11 ± 0.49
MAE_{550}, $m^2\,g^{-1}$ C	0.082 ± 0.30	0.19 ± 0.11	0.17 ± 0.083	0.13 ± 0.069	0.094 ± 0.054	0.29 ± 0.075
Å	6.32 ± 0.58	5.37 ± 0.57	5.47 ± 0.67	5.57 ± 0.39	6.06 ± 0.54	4.53 ± 0.21

[a] Light absorption coefficient of SEOC after the first extraction; [b] sum of SEOC absorption in 1st and 2nd extracts.

Table 3. Comparisons of light-absorbing properties of ambient PM$_{2.5}$ extracts in DMF and MeOH derived from duplicate Q$_f$–Q$_b$ data ($N = 109$).

	DMF			MeOH[a]		
	Median	Mean ± std	Range	Median	Mean ± std	Range
Abs$_{365}$, Mm^{-1}	6.99	8.42 ± 5.40	1.14–30.8	5.59	6.43 ± 4.66	0.38–29.6
MAE$_{365}$, m^2 g^{-1}C	1.13	1.20 ± 0.49	0.34–2.45	0.91	1.03 ± 0.58	0.089–2.49
Å	5.21	5.25 ± 0.64	3.21–6.82	6.49	6.81 ± 1.64	4.34–11.3

[a] Data for MeOH extracts were obtained from Xie et al. (2022).
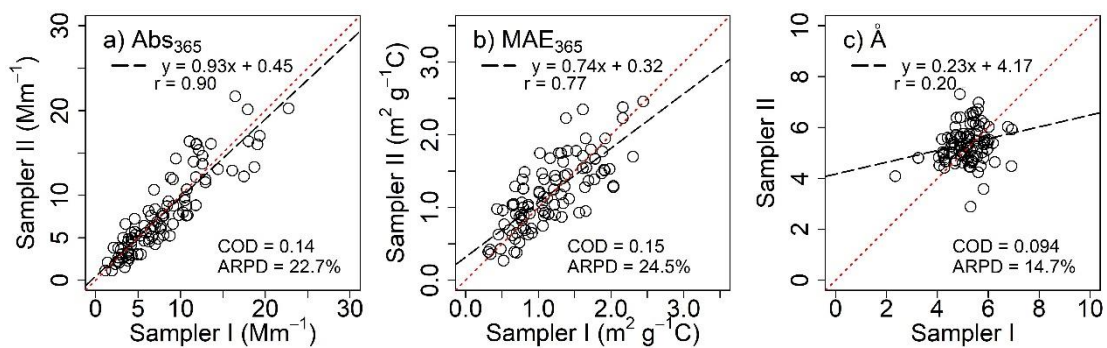
Figure 1

Figure 1. Comparisons between collocated measurements for light-absorbing properties of $PM_{2.5}$ extracts in DMF after Q_b corrections.
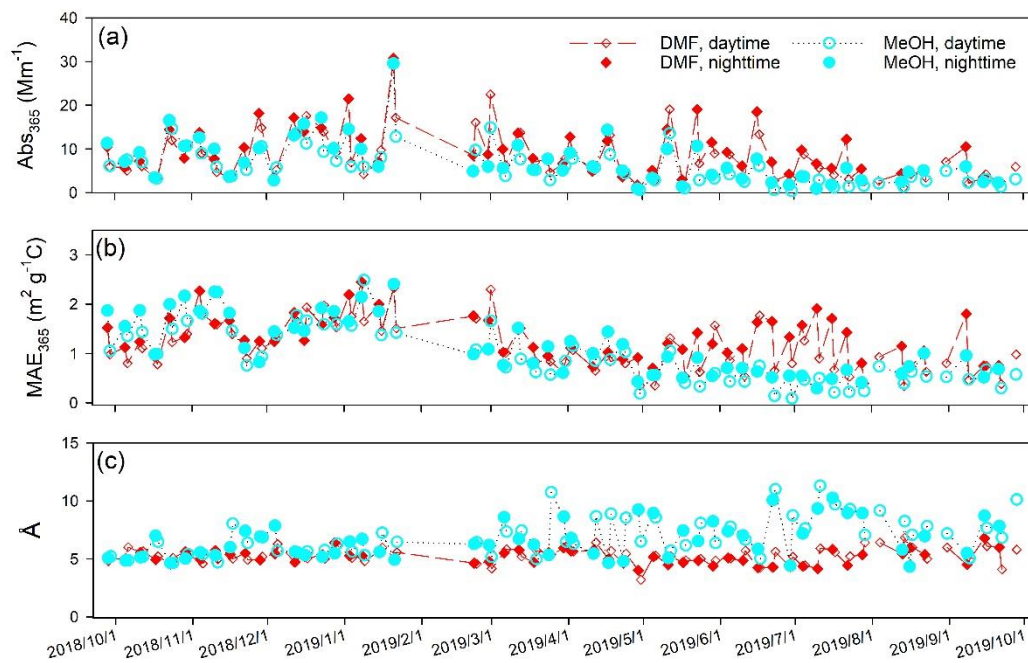
Figure 2

Figure 2. Time series comparisons of light-absorbing properties of DMF and MeOH extracts using artifact-corrected data. MeOH extract data were obtained from Xie et al. (2022).
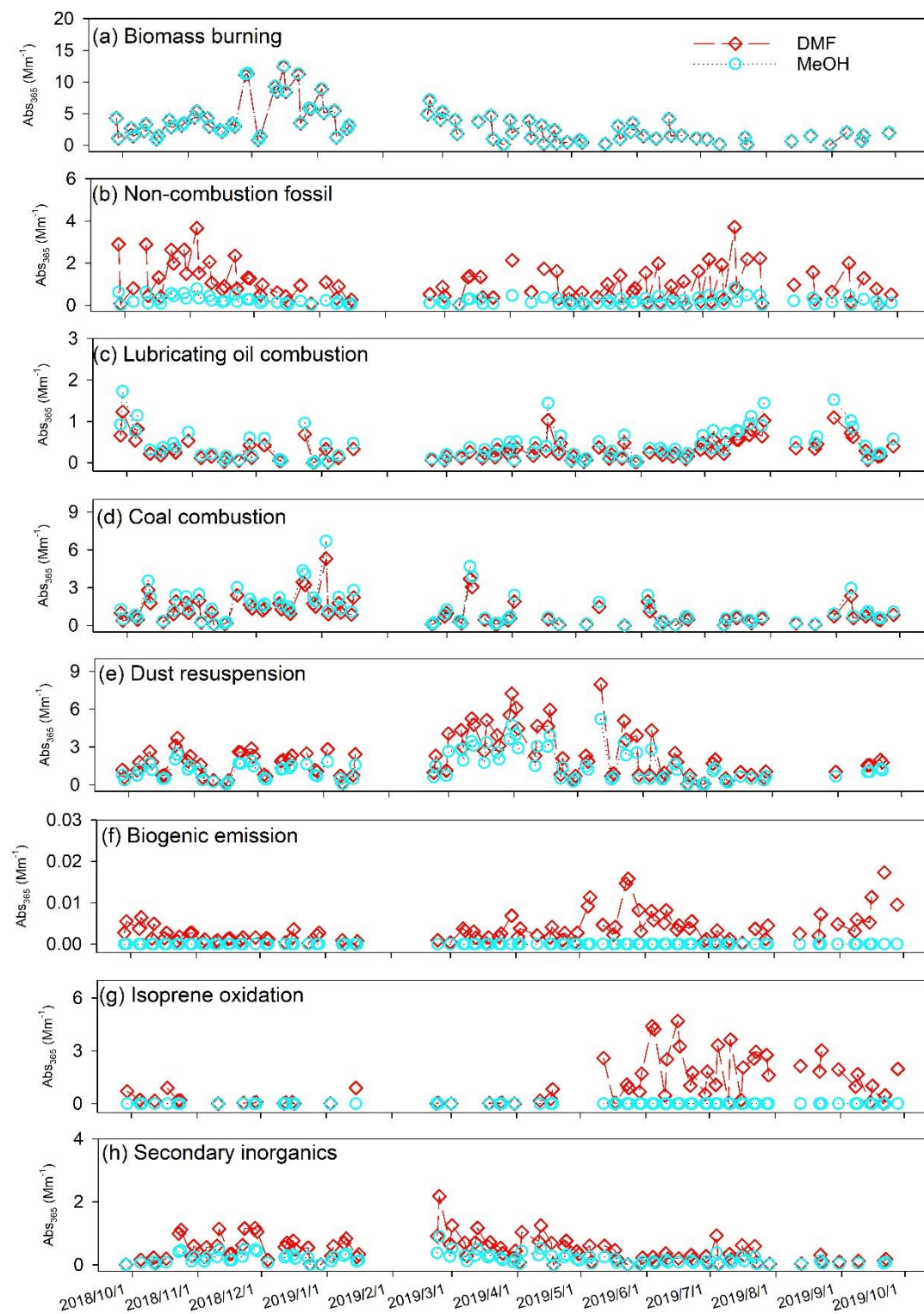
Figure 3

Figure 3. Time series of factor contributions to Abs$_{365}$ of DMF and MeOH extracts of ambient PM$_{2.5}$ samples.